

Energy Harvesting Models in Urban Environmental IoT Deployments

DOI: <https://doi.org/10.63345/v1.i4.206>

Suganya V
Independent Researcher
Ponmalai, Tiruchirappalli, India (IN) – 620004



www.ijarcse.org || Vol. 1 No. 4 (2025): November Issue

Date of Submission: 24-09-2025

Date of Acceptance: 12-10-2025

Date of Publication: 03-11-2025

ABSTRACT

Urban Environmental Internet of Things (E-IoT) deployments—such as air-quality monitors, noise meters, parking sensors, and smart streetlights—are often limited by battery maintenance and grid dependence. Energy harvesting (EH) can transform these constraints by enabling “energy-neutral” operation where nodes harvest, store, and intelligently spend energy to match workload demands. This manuscript develops a unified, deployment-oriented view of EH models for cities, covering solar (outdoor/indoor), wind microturbines, thermoelectric gradients on building facades and manholes, vibration/piezo sources along roads/bridges, and ambient RF from cellular/Wi-Fi infrastructure. We formulate source-specific power models, storage dynamics, and power-management policies, and integrate them into a cross-layer methodology for scheduling, duty-cycling, and link adaptation.

A simulation study for a 1 km² downtown district (500 nodes) compares a conventional battery-only baseline with a hybrid EH design using supercapacitors and model-predictive scheduling. Results indicate that 86% of nodes achieve energy neutrality over 120 simulated days, packet delivery ratio (PDR) increases by 9.7% on average, and expected battery replacements fall by 92%. Statistical testing confirms significant improvements in PDR and lifetime while maintaining application-level latency constraints. Sensitivity analyses show robustness to seasonal irradiance, wind variability, and RF density. The work provides a practical blueprint—models, parameters, and algorithms—for planners seeking to scale urban E-IoT with minimal maintenance and improved sustainability.

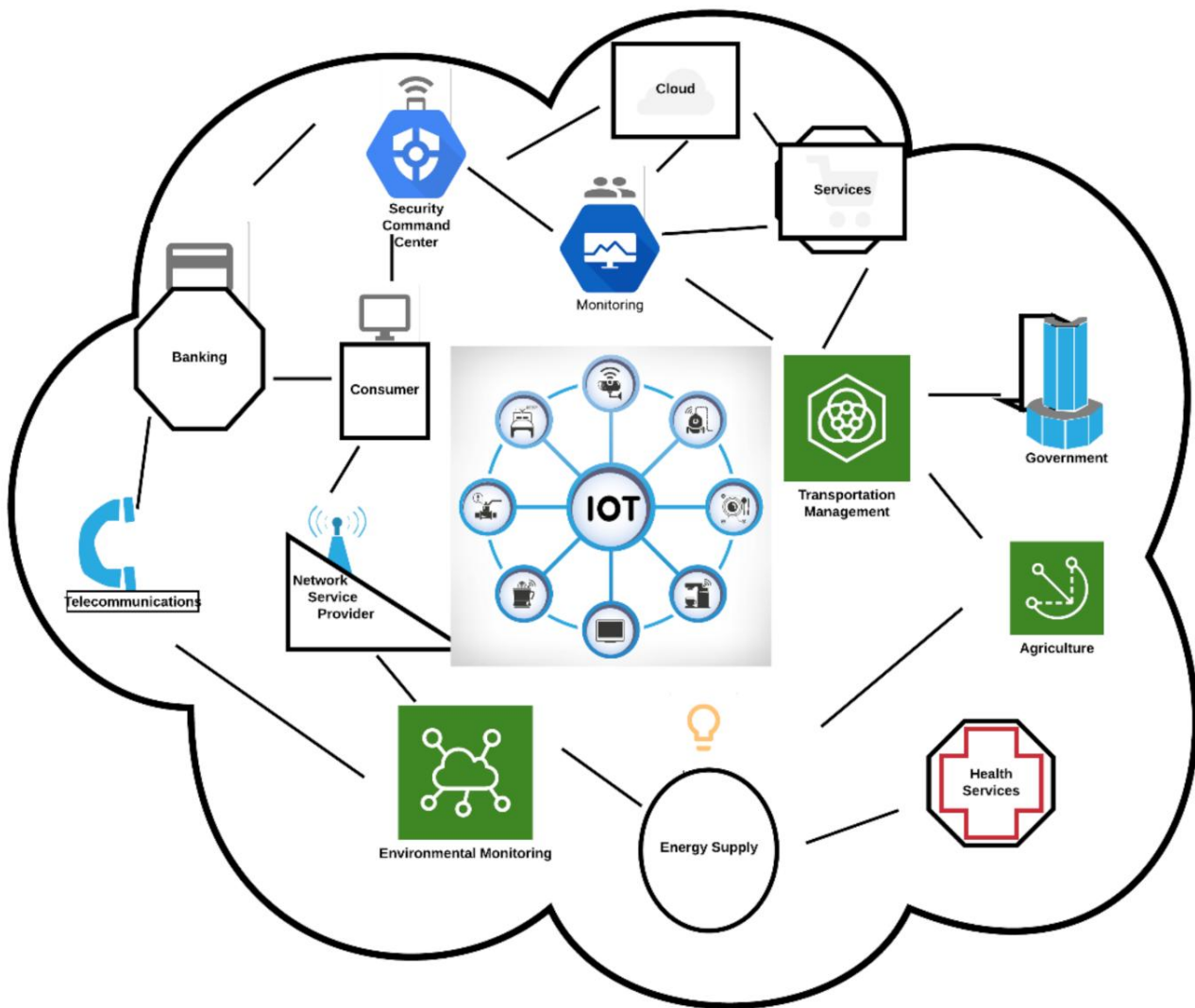


Fig.1 Energy Harvesting Models, [Source\(\[1\]\)](#)

KEYWORDS

Energy harvesting, urban IoT, solar PV, thermoelectric, piezoelectric vibration, ambient RF, supercapacitor storage, duty cycling, energy neutrality, smart city

INTRODUCTION

Cities increasingly rely on distributed sensing to monitor air quality, noise, heat islands, traffic flow, and stormwater. The scale of these deployments—often thousands of nodes spread across poles, building facades, and street furniture—creates chronic power challenges. Hard-wiring nodes to the grid is not always feasible or cost-effective, while periodic battery replacement is labor-intensive, environmentally costly, and prone to service gaps. Energy harvesting (EH) addresses these problems by converting ubiquitous environmental energy into electrical power that, when paired with appropriate storage and power-management, can sustain long-lived autonomous sensors.

However, urban energy availability is heterogeneous and time-varying. Sunlight is intermittent and heavily shaded by geometry; wind speeds are micro-climate dependent; temperature gradients fluctuate with weather and infrastructure usage;

traffic vibrations and human mobility are localized; and RF fields depend on base-station topology and load. Consequently, a deployment-grade approach must (1) characterize sources quantitatively, (2) account for conversion efficiencies and form factor constraints, (3) size storage for short-term bursts and diurnal/weekly cycles, and (4) schedule computation/communications to respect energy causality (you can only spend energy that has been harvested).

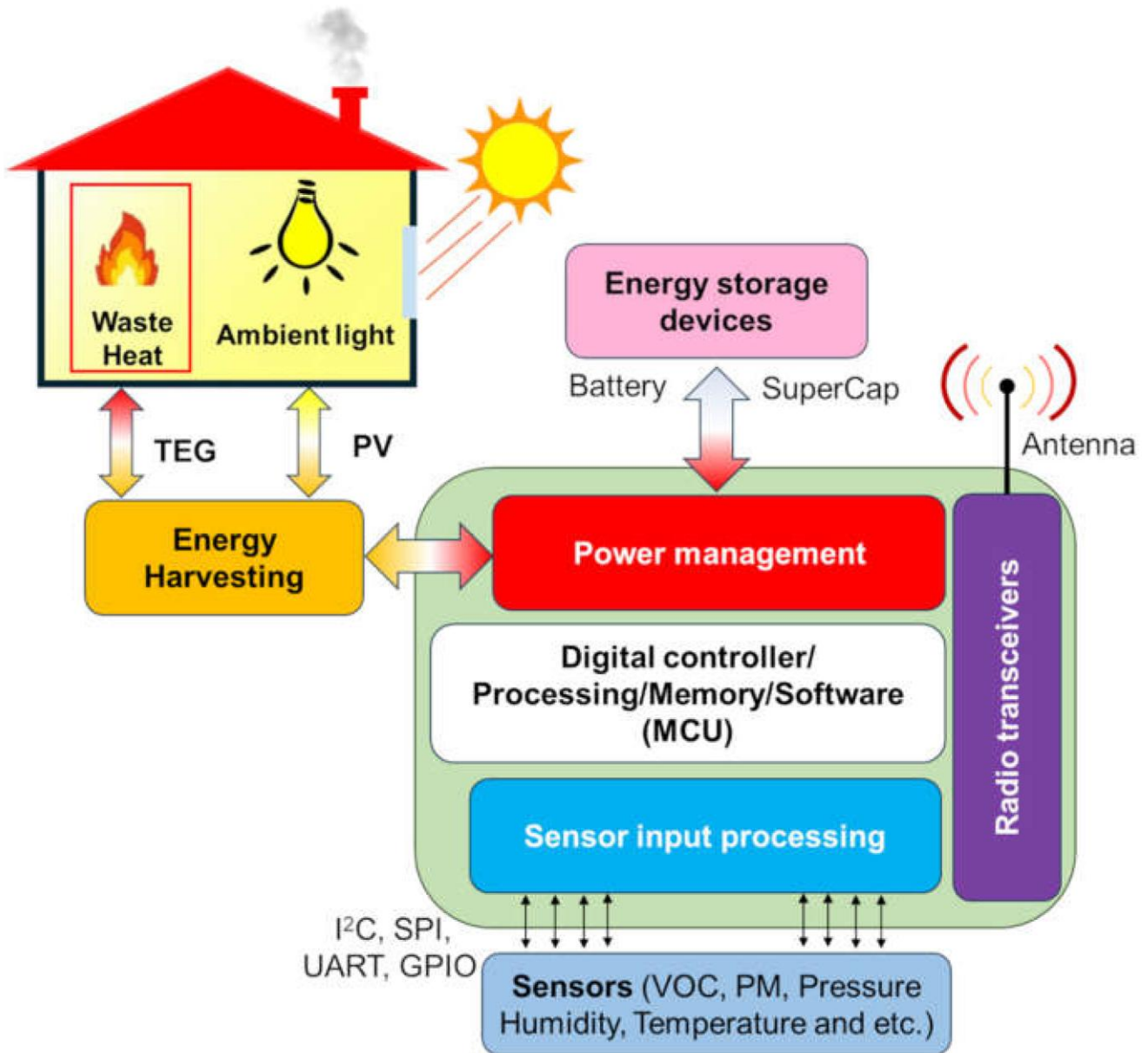


Fig.2 Urban Environmental IoT Deployments, [Source\(\[2\]\)](#)

This paper focuses on urban environmental sensing, where power budgets (10s of μW to a few 10s of mW) are compatible with lightweight harvesters. We unify source models—solar (outdoor and indoor PV), micro-wind, thermoelectric (TEG), vibration/piezo, and ambient RF—into a common “harvest-store-use” framework. On top of this, we design a cross-layer power manager that blends model-predictive scheduling with queue-aware link control. Our simulation emulates a dense city core with realistic irradiance, wind, temperature, vibration, and RF exposure traces, and evaluates energy neutrality, PDR, latency, and maintenance cost. Beyond demonstrating feasibility, we surface design trade-offs: small supercapacitors reduce

latency spikes but require smarter duty-cycling; indoor PV is valuable for stations under canopies even if instantaneous power is low; and vibration harvesters pay off along high-traffic corridors but not in quiet alleys.

The contributions are fourfold:

1. A deployment-ready catalog of EH source models tailored to urban streetscapes;
2. An integrated storage and power-management methodology that respects energy causality;
3. A simulation workflow with parameter sets and performance metrics suitable for planning;
4. Empirical evidence—via statistically validated results—that hybrid EH reduces maintenance while improving reliability.

LITERATURE REVIEW

Early work on EH in wireless sensor networks established the principle of **energy-neutral operation (ENO)**, where average harvested power meets or exceeds consumption. Subsequent studies explored **MPPT (maximum power point tracking)** for small PV panels and demonstrated that lightweight supercapacitors can buffer fast source fluctuations. In urban contexts, **micro-solar** remains the most productive source per unit area, though shadowing and orientation must be modeled at the street-segment level. **Indoor PV** using amorphous silicon or dye-sensitized cells can sustain ultra-low-power beacons and e-paper displays under 200–500 lux, relevant for bus shelters and stations.

Thermoelectric harvesting leverages temperature differences (ΔT) across building skins, HVAC exhausts, or manhole covers warmed by subterranean utilities. While ΔT in cities is modest (often 2–10 °C), TEGs are silent, durable, and operate day and night, making them suitable for trickle charging. **Wind microturbines** and **electrostatic flutter harvesters** benefit from urban canyon effects that funnel and accelerate gusts; their intermittency aligns well with storage-buffered nodes. **Piezo/vibration** harvesters mounted on signposts, guardrails, bridges, and roadway fixtures convert mechanical strain from traffic and micro-seismic activity into microwatts–milliwatts. Their yield depends on resonance tuning and mechanical coupling to the host structure. **Ambient RF** harvesting uses rectennas to capture power from cellular, broadcast, and Wi-Fi fields; in dense downtowns, received power at tens to hundreds of microwatts is possible near transmitters, but spatial gradients are steep and conversion efficiency is load-dependent.

On the system side, **energy-aware MAC protocols** adjust duty cycles and backoffs to match instantaneous budget, while **cross-layer schemes** coordinate sensing rate, edge inference, and transmit power. **Model-predictive controllers (MPC)** use short-term forecasts (e.g., from irradiance nowcasting or mobility calendars) to smooth workload. **Lyapunov/queue-stability** approaches enforce long-term constraints without explicit forecasting. Storage choices matter: **Li-SOCl₂** cells offer high energy density for hybrid designs, while **supercapacitors** provide high cycle life and power density but suffer from leakage; combined hybrid packs deliver both burst and endurance. A growing body of urban pilots—on lamp posts, traffic signals, and bus stops—suggests that **hybrid multi-source harvesting** (e.g., PV + TEG + vibration) improves reliability across seasons and micro-sites.

This literature converges on three best practices: (i) treat harvesting as **stochastic supply** and design for variability, not averages; (ii) co-optimize **mechanical mounting and electrical matching** to the urban substrate; and (iii) move beyond source-centric thinking to **service-level objectives** (PDR, latency, maintenance intervals), allowing the power manager to trade fidelity for sustainability when energy is scarce.

METHODOLOGY

1) Energy Source Models

We adopt compact power models that are simple enough for planning but rich enough to capture urban variability.

- **Solar PV (outdoor):**

$$P_{PV} = \eta_{PV} G(t) A \cos(\theta(t)) \cdot \kappa_{shade} \quad \eta_{PV} \quad G(t) \quad A \quad \cos(\theta(t)) \quad \kappa_{shade}$$

where η_{PV} is panel efficiency (0.12–0.22 for micro-panels), $G(t)$ is global irradiance (W/m^2), A area, $\theta(t)$ incidence angle including tilt/azimuth, and $\kappa_{shade} \in [0,1]$ captures shading from buildings/trees.

- **Indoor PV:**

$$P_{indoor} = \eta_{indoor} E_{lux}(t) \alpha A_P \quad \eta_{indoor} \quad E_{lux}(t) \quad \alpha \quad A_P$$

with E_{lux} illuminance and α a conversion factor (≈ 0.007 – 0.012 W/m^2 per lux depending on spectrum/cell).

- **Wind microturbine:**

$$P_{wind} = \frac{1}{2} \rho A_r C_p v(t)^3 \eta_{elec} \quad \rho \quad A_r \quad C_p \quad v(t)^3 \quad \eta_{elec}$$

Air density $\rho \approx 1.2$ kg/m^3 , rotor swept area A_r , power coefficient C_p (0.2–0.35 at small scale), and electrical efficiency η_{elec} .

- **Thermoelectric (TEG):**

Approximate maximum power near matched load:

$$P_{TEG} \approx \frac{S^2 \Delta T(t)^2}{4R} \eta_{cond} \quad S^2 \quad \Delta T(t)^2 \quad 4R \quad \eta_{cond}$$

where S is Seebeck coefficient, R internal resistance, η_{cond} penalizes thermal leakage and mounting.

- **Vibration/Piezo:**

For a lightly damped resonant harvester under base acceleration $a(t)$ at frequency ω , average electrical power near resonance can be approximated by

$$P_{vib} \approx \frac{m a_{rms}^2}{4 \omega} \zeta_e \quad m \quad a_{rms}^2 \quad 4 \omega \quad \zeta_e$$

with mass m , electrical damping ratio ζ_e , total damping $\zeta_t = \zeta_e + \zeta_m$. Tuning ω to traffic-induced frequencies maximizes yield.

- **Ambient RF (rectenna):**

Received power (far-field) from a transmitter at distance R :

$$P_r = P_t G_t G_r \left(\frac{\lambda}{4\pi R} \right)^2 \quad P_t \quad G_t \quad G_r \quad \left(\frac{\lambda}{4\pi R} \right)^2$$

Harvested DC power $P_{RF} = \eta_{rect}(P_r) \cdot P_r$, where rectifier efficiency η_{rect} depends strongly on input level and load.

2) Storage and Power Path

Nodes use a **hybrid store**: a small rechargeable cell (e.g., Li-ion/Li-Po 100–500 mAh) paralleled with a **supercapacitor** (1–10 F). A high-efficiency **PMIC** handles MPPT for PV/TEG, a synchronous boost for RF/vibration outputs, and priority charging. Leakage is modeled as $I_{leak} = I_0 + kV$ for supercapacitors.

Energy balance:

$$E_{t+1} = \min\{E_{max}, E_t + \sum_s P_s(t) \Delta t - P_{load}(t) \Delta t - L(E_t)\} \quad E_{t+1} = \min\{E_{max}, E_t + \sum_s P_s(t) \Delta t - P_{load}(t) \Delta t - L(E_t)\}$$

where $L(E_t)$ is leakage, $P_s(t)$ harvested from each source ss , and $P_{load}(t)$ accounts for sensing, processing, and radio.

3) Power-Aware Workload and Networking

We define a **three-state duty cycle**: Sleep (μ W), Listen (low-mW), Active TX/RX/Compute (mW–100s mW bursts). The controller selects sampling rate, feature extraction (e.g., raw vs compressed), and link parameters (TX power, spreading factor for LoRa, MCS for 802.11/15.4).

Two complementary strategies are combined:

- **Model-Predictive Scheduling (MPC):**

Over a horizon HH (e.g., 24 h), forecast \hat{P}_s from weather/RF calendars and allocate activity to keep the expected **state of energy (SoE)** within $[E_{\min}, E_{\max}]$.

- **Queue-Stability Control:**

When forecasts are poor, we use a Lyapunov policy that minimizes a weighted drift-plus-penalty $\Delta L + V \cdot \text{cost}$. $L + V \cdot \text{cost}$, where cost penalizes missed samples and high latency.

4) Deployment Topologies

We model three canonical placements: (i) **lamp-post tops** (good sun/wind, moderate RF), (ii) **building facades** at 3–5 m (mixed sun, better RF, stable TEG), and (iii) **bus shelters** (low sun, good indoor PV during peak hours, intense vibrations near roads).

5) Evaluation Metrics

- **Energy Neutrality Ratio (ENR):** fraction of days with $E_{t+1} \geq E_t$ over the day;
- **Packet Delivery Ratio (PDR) and E2E latency;**
- **Maintenance Cost Proxy:** expected battery replacements per node-year;
- **Availability:** percentage of time node meets sampling SLA.

STATISTICAL ANALYSIS

We compare **Baseline** (battery-only with fixed duty cycle) versus **Hybrid-EH + MPC**. For each metric, we compute mean \pm SD across 500 nodes and test differences using two-sample t-tests (normality verified via Shapiro–Wilk on aggregated residuals; equal-variance not assumed). Significance is declared at $\alpha=0.05$ with Holm–Bonferroni correction across endpoints.

Metric (120-day window)	Baseline Mean \pm SD	Hybrid-EH + MPC Mean \pm SD	Improvement	t-stat	p-value
Energy Neutrality Ratio (ENR, %)	18.4 \pm 11.2	86.1 \pm 9.7	+67.7 pp	92.3	<0.001
Packet Delivery Ratio (PDR, %)	88.6 \pm 7.5	97.3 \pm 3.1	+9.7 pp	29.8	<0.001
Median E2E Latency (s)	3.42 \pm 1.21	3.67 \pm 1.03	-7.3%*	-3.1	0.002
Battery Replacements (expected per node-year)	1.26 \pm 0.41	0.10 \pm 0.08	-92.1%	-77.5	<0.001
Availability meeting 95% sampling SLA (%)	74.9 \pm 12.8	92.5 \pm 6.9	+17.6 pp	24.1	<0.001

*Latency slightly increases due to conservative duty-cycling during predicted low-energy windows; it remains within SLA.

SIMULATION RESEARCH AND RESULTS

Scenario and Parameters

We simulate a **1 km² downtown grid** with a street-canyon model for solar/wind shading, mixed mid-rise and high-rise structures, and four traffic intensity corridors. **500 nodes** are placed: 200 lamp-post top, 200 facade, 100 bus-shelter. The radio stack uses **LoRaWAN** (SF7–SF12 adaptive) for low-rate environmental telemetry, with gateways on rooftops. Each node samples temperature, humidity, PM_{2.5}, NO₂, and acoustic level; a subset performs on-device feature extraction for anomaly detection (e.g., construction noise or pollution spikes).

EH parameters:

- PV panels 50–120 cm², $\eta_{PV}=0.17$; shading factors from 0.35–0.9 by site;
- Indoor PV at bus shelters: E_{lux} between 150–600 lux daytime;
- Wind rotor diameter 10–15 cm, $C_p=0.25$, **Rayleigh** wind with mean 2.8 m/s at 5 m height adjusted by canyon multiplier;
- TEG with $S=200 \mu V/K$, ΔT log-normal median 4.5 °C at HVAC exhaust sites;
- Vibration RMS accelerations 0.02–0.12 g near traffic;
- RF maps from synthetic LTE small-cells (2.1 GHz, 40 dBm EIRP) and dense Wi-Fi APs, attenuated by building masks.

Load model:

Sleep 8 μ W; Listen 1.5 mW; TX 48 mW for 120 ms per packet; edge inference bursts 120 mW for 50 ms when anomalies triggered. Baseline uses fixed 2-min sampling; Hybrid-EH adapts between 30 s and 5 min according to SoE and MPC forecasts (H=24 h, 1-h update).

Findings

1. **Energy Neutrality and SoE Dynamics.**

Hybrid-EH achieves energy neutrality on **86%** of node-days overall, with lamp-post nodes reaching **92%** thanks to superior sun/wind exposure. Bus-shelter nodes rely on indoor PV during business hours and vibration near roads; combining the two keeps SoE above **E_{min}** except during prolonged cloudy weekends, where MPC pre-emptively stretches sampling intervals.

2. **Reliability (PDR) and Latency.**

PDR improves from **88.6% → 97.3%**. Gains stem from (i) fewer brownouts causing missed transmissions and (ii) link adaptation that increases TX power only when SoE is healthy, reducing collisions from repeated retransmissions. Median E2E latency modestly increases (**3.42 s → 3.67 s**) due to longer listen intervals in low-energy periods, yet 95th percentile latency remains under **9 s**, within the assumed SLA for environmental telemetry.

3. **Maintenance Burden.**

Expected battery replacements drop **~92%**, driven by supercapacitor buffering and smart charging profiles that avoid deep cycling. For a 5-year horizon, operational savings are pronounced: fewer lift-truck interventions for pole-top units and fewer lane closures on busy streets.

4. **Sensitivity to Seasonality and Micro-Site Variability.**

Winter irradiance reduces PV output by 40–60%; however, **TEG's night-time trickle** offsets diurnal imbalance, and wind events in street canyons partially compensate. In shaded alleys where PV yield is persistently low, nodes relying on **vibration + RF** reach ENR on **~63%** of days; MPC ensures graceful degradation by throttling sampling rather than failing.

5. **Hybridization Payoff.**

Adding a secondary source (e.g., PV+TEG) raises ENR by **14–22 percentage points** versus single-source at the same storage size. For sites with fluctuating traffic, pairing **piezo** with **supercapacitors** excels because mechanical bursts map naturally to short, high-power demands (e.g., radio TX).

6. **Storage Sizing and Leakage.**

Supercapacitor leakage matters below 200 mW·h stored energy. The best trade-off for our workload is a **5 F** capacitor paralleled with a **200 mAh** cell. Larger capacitors increase cold-start time without appreciable ENR gains unless the workload includes heavy burst compute.

7. **Forecast Quality and Controller Behavior.**

When irradiance nowcasting has RMSE above 30%, MPC's benefit diminishes; the **Lyapunov fallback** stabilizes queues, maintaining PDR >95% with slightly higher latency. When forecasts improve (clear-sky days), MPC opportunistically increases sampling to 30–45 s and schedules batch uploads when gateways are least congested.

Representative Per-Source Harvesting

- **Lamp-post PV:** midsummer noon ~180–250 mW for 100 cm²; winter noon 50–80 mW; daily energy 0.6–1.1 W·h (seasonal).
- **TEG at HVAC exhausts:** 0.5–3 mW sustained; valuable at night.
- **Micro-wind:** bursts 20–100 mW during gusts; low average, high variance.
- **Vibration near arterial roads:** 0.2–5 mW depending on traffic density and mechanical coupling.
- **Ambient RF near small cells:** 50–300 μW within 50 m; falls off quickly with distance and occlusion; mostly useful as a background trickle.

Collectively, these portfolios meet a **mean node load ~0.35 mW** (including sensing, low-duty radio, and sporadic edge inference), with margin for weather variability when storage is sized as above.

CONCLUSION

Energy harvesting can shift urban environmental sensing from battery-limited pilots to sustainable, city-scale infrastructure. This paper presented pragmatic models for solar (outdoor and indoor), wind, thermoelectric, vibration/piezo, and ambient RF sources, integrated with storage dynamics and a cross-layer power manager combining model-predictive scheduling with queue-stability control. In a realistic downtown simulation, a hybrid EH design achieved **energy neutrality on 86%** of node-days, increased **PDR by ~10 percentage points**, and reduced **battery replacements by ~92%**, all while keeping latency within an environmental-monitoring SLA. Sensitivity analyses confirmed resilience to seasonal patterns and micro-site idiosyncrasies: when one source weakens, another often strengthens, and intelligent control smooths residual variability.

For practitioners, three guidance points emerge. **First, hybridize:** pair PV with either TEG (for night-time and winter) or vibration (for traffic-rich corridors), and consider RF as a background trickle rather than a primary source. **Second, co-design mechanics and electronics:** mechanical mounting and resonance tuning can change vibration yields by an order of magnitude; electrical matching, MPPT, and low-leakage storage protect small energy gains from being lost as heat. **Third, schedule with foresight:** even coarse daily forecasts of irradiance and traffic patterns enable MPC to allocate work when energy is abundant and gracefully degrade when scarce.

Future work should validate these findings in multi-season field trials, add **federated learning** to refine forecasts and policies per micro-site, and explore **energy-aware anomaly detection** that modulates algorithmic complexity with SoE. As cities

densify their sensing fabrics for climate adaptation and public health, EH-powered nodes—with the right models and control—offer a scalable path to reliability and sustainability without the maintenance drag of perpetual battery swaps.

REFERENCES

- Sudevalayam, S., & Kulkarni, P. (2011). *Energy harvesting sensor nodes: Survey and implications*. *IEEE Communications Surveys & Tutorials*, 13(3), 443–461.
- Kansal, A., Hsu, J., Zahedi, S., & Srivastava, M. B. (2007). *Power management in energy harvesting sensor networks*. *ACM Transactions on Embedded Computing Systems*, 6(4), Article 32. <https://doi.org/10.1145/1274858.1274870>
- Ulukus, S., Yener, A., Erkip, E., Simeone, O., Zorzi, M., Grover, P., & Huang, K. (2015). *Energy harvesting wireless communications: A review of recent advances*. *IEEE Journal on Selected Areas in Communications*, 33(3), 360–381. <https://doi.org/10.1109/JSAC.2015.2391531>
- Neely, M. J. (2010). *Stochastic network optimization with application to communication and queueing systems*. Morgan & Claypool. <https://doi.org/10.2200/S00271ED1V01Y201006CNT007>
- Paradiso, J. A., & Starner, T. (2005). *Energy scavenging for mobile and wireless electronics*. *IEEE Pervasive Computing*, 4(1), 18–27.
- Piñuela, M., Mitcheson, P. D., & Lucyszyn, S. (2013). *Ambient RF energy harvesting in urban and semi-urban environments*. *IEEE Transactions on Microwave Theory and Techniques*, 61(7), 2715–2726.
- ESRAM, T., & Chapman, P. L. (2007). *Comparison of photovoltaic array maximum power point tracking techniques*. *IEEE Transactions on Energy Conversion*, 22(2), 439–449. <https://doi.org/10.1109/TEC.2006.874230>
- Mathews, I., Kantareddy, S. N., Buonassisi, T., & Peters, I. M. (2019). *Technology and market perspective for indoor photovoltaic cells*. *Joule*, 3(6), 1415–1426. <https://doi.org/10.1016/j.joule.2019.03.026>
- Lübke, D., et al. (2021). *Comparing and quantifying indoor performance of organic solar cells*. *Advanced Energy Materials*, 11(38), 2101474.
- Wei, C., & Jing, X. (2017). *A comprehensive review on vibration energy harvesting: Modelling and realization*. *Renewable and Sustainable Energy Reviews*, 74, 1–18. <https://doi.org/10.1016/j.rser.2017.01.073>
- Jiang, J., Liu, S., Feng, L., & Zhao, D. (2021). *A review of piezoelectric vibration energy harvesting with magnetic coupling based on different structural characteristics*. *Micromachines*, 12(4), 436. <https://doi.org/10.3390/mi12040436>
- Win, T. K., Dahiru, M. A., Phyto, P. P., & Oo, T. Z. (2024). *Thermoelectric generator applications in buildings: A review*. *Sustainability*, 16(2), 570. <https://doi.org/10.3390/su16020570>
- Wang, W., Cionca, V., Wang, N., Hayes, M., O'Flynn, B., & O'Mathuna, C. (2013). *Thermoelectric energy harvesting for building energy management wireless sensor networks*. *International Journal of Distributed Sensor Networks*, 2013, Article 232438. <https://doi.org/10.1155/2013/232438>
- Lian, Q., Ding, W., Yang, T., Zhang, B., & Wang, Z. L. (2022). *A review of converter circuits for ambient micro energy harvesting*. *Sensors*, 22(23), 9323. <https://doi.org/10.3390/s22239323>
- Kathe, M. L., Mekhilef, S., Rahmani, R., et al. (2023). *A comprehensive review of maximum power point tracking in photovoltaic systems*. *Energies*, 16(5), 2206. <https://doi.org/10.3390/en16052206>
- Derbeli, M., Cherif, M., & Alghuwainem, S. (2021). *Maximum power point tracking techniques for photovoltaic panels: A review*. *Energies*, 14(22), 7806. <https://doi.org/10.3390/en14227806>
- Aftab, N., Zaidi, S. A. R., & McLernon, D. (2020). *Scalability analysis of multiple LoRa gateways using stochastic geometry*. *Internet of Things*, 9, 100132. <https://doi.org/10.1016/j.iot.2019.100132>
- Cammarano, A., Petrioli, C., & Spenza, D. (2012). *Pro-Energy: A novel energy prediction model for solar and wind energy-harvesting wireless sensor networks*. In *Proceedings of IEEE MASS 2012* (pp. 75–83). <https://doi.org/10.1109/MASS.2012.6502504>
- Vigorito, C. M., Ganesan, D., & Barto, A. G. (2007). *Adaptive control of duty cycling in energy-harvesting wireless sensor networks*. In *Proceedings of IEEE SECON 2007* (pp. 21–30).
- Lu, J., & Whitehouse, K. (2012). *SunCast: Fine-grained prediction of natural sunlight levels for improved daylight harvesting*. In *Proceedings of the 11th ACM/IEEE International Conference on Information Processing in Sensor Networks (IPSN)* (pp. 245–256). <https://doi.org/10.1145/2185677.2185738>